

Photoinduced Intramolecular Charge Transfer in Donor–Acceptor Substituted Tetrahydropyrenes[†]

S. Sumalekshmy and K. R. Gopidas*

Photosciences and Photonics Division, Regional Research Laboratory (CSIR), Trivandrum 695 019, India

Received: December 9, 2002; In Final Form: October 29, 2003

Two novel donor–acceptor-substituted tetrahydropyrene derivatives (**1** and **2**, Chart 1) were synthesized and photophysical properties investigated in solvents of different polarities. These studies revealed the existence of an intramolecular charge transfer (ICT) excited state in these molecules. The fluorescence lifetime and quantum yield measurements revealed that emission occurs from a planar ¹CT state in all the solvents. The solvent-dependent Stokes shift values for **1** and **2** were analyzed by the Lippert–Mataga equation and Liptay's modified equation to obtain the excited-state dipole moment values. The CT nature of the emitting states is further confirmed by studies in acidic medium. Change of pH results in well-separated LE and CT fluorescence and absorption bands. It is suggested that this property can be utilized for pH-sensing applications.

Introduction

Photoinduced intramolecular charge transfer (ICT) plays a key role in the photophysics of donor (D)–acceptor (A)-substituted conjugated systems.^{1–15} Molecules of the type D– π –A, where the donor and acceptor groups are connected to the ends of a conjugated system, exhibit large changes in dipole moment ($\Delta\mu$) upon excitation due to a photoinduced ICT process. The extent of CT depends on the nature of the D and A groups and the length of the π system. Conformational dynamics of the donor and acceptor fragments can also significantly influence the photochemistry of such systems. For example, the photoinduced CT in dimethylaminobenzonitrile (DMABN) and its dual emission has been under controversial discussion for over 20 years.^{16–24} It has been suggested that the dual emission is due to a conformational twisting in the excited state.^{24,25} An alternate model, involving pseudo-Jahn–Teller interaction of two energetically close-lying ¹L_a- and ¹L_b-type benzenic states, is also suggested.^{21,22}

Lengthening the π system in D– π –A is expected to increase the $\Delta\mu$ term, resulting in substantial redshifts of the fluorescence spectrum. In this context, photoinduced CT processes in several D–A-substituted biphenyls have been explored.^{26–45} The phenyl groups in biphenyl are not coplanar, and the twist angle depends on the substituents in the molecule. It has been worked out that in the ground state the twist angle lies between 15° and 40°, whereas in the S₁ state planar geometry is preferred.³³ The photophysics of D–A biphenyls depend strongly on the twist angle and also on solvent polarity, making the assignment of the electronic states very difficult. Depending on the D and A groups, the biphenyls have S₁ states possessing (1) ¹L_a- or ¹L_b-type character,⁴² (2) solvent polarity dependent nonradiative intramolecular channels,⁴³ or (3) nonradiative channels due to specific solvent interactions.⁴⁴ To understand these processes in more detail, it is necessary to study biphenyl systems with

rigid structure where rotation about the central single bond (C₁–C_{1'}) is restricted or absent. A few such systems have been examined.

Photoinduced ICT processes in a series of differently twisted 4-*N,N*-dimethylamino-4'-cyanobiphenyls were investigated in great detail by Rettig and co-workers.^{33–37} The dipole moments, radiative rates, and torsional relaxations in the excited state were analyzed by comparison with absorption spectra and interannular twist angle dependent complete neglect of differential overlap/spectroscopic (CNDO/S) calculations. It was concluded that the electronic nature of these molecules could be explained in terms of a composite molecular model with the dimethylaminophenyl moiety acting as the donor unit and the cyanophenyl moiety acting as the acceptor unit. The first excited singlet state in these D–A biphenyls is an emissive intramolecular ¹CT state irrespective of solvent and twist angle. In the case of a strongly twisted biphenyl derivative, a secondary intramolecular process to a more relaxed species occurs after the initial CT process.

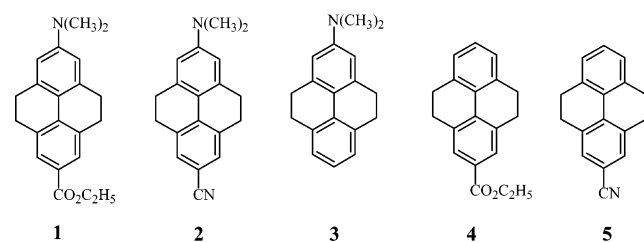
This paper investigates the ICT processes in D–A-substituted tetrahydropyrenes **1** and **2** (Chart 1). Tetrahydropyrenes can be considered as rigid biphenyl derivatives. Although the ICT processes in a few biphenyl systems have been studied using steady-state and time-resolved fluorescence spectroscopy as well as theoretical methods,^{26–45} little is known about this process in tetrahydropyrene derivatives. This is most probably due to the difficulties involved in the synthesis of these molecules. The torsional angle (φ) between the phenyl units in these systems is 14° (from AM1 calculation), which is between the values reported for the well-studied biphenyl systems 2-(dimethylamino)-7-cyanofluorene ($\varphi = 0^\circ$) and 4-(dimethylamino)-4'-cyanobiphenyl ($\varphi = 39^\circ$).³³ To have a better understanding of the photophysical properties of **1** and **2**, model compounds **3**–**5** were prepared and their photophysical properties were also investigated.

We have observed that the fluorescence maxima of **1** and **2** are very much dependent on the polarity of the solvent due to the ICT nature of the transitions. Since the nitrogen lone pair of the dimethylamino group is involved in the CT process, addition of proton acids leads to substantial changes in the absorption and fluorescence spectra of **1** and **2**. In the presence

[†] This is publication number PPD-(RRLT)-162 from the Photosciences and Photonics Division, Regional Research Laboratory (CSIR) Trivandrum.

* Author to whom correspondence may be addressed. E-mail: gopidaskr@rediffmail.com.

CHART 1



of proton acids, **1** and **2** exhibit pH-dependent dual absorption and dual emission. We have explored this feature in order to evaluate the potential of these molecules as pH sensors.

Experimental Section

General Techniques. All melting points are uncorrected and were determined using a Mel-Temp melting point apparatus. ^1H and ^{13}C NMR spectra were obtained using a 300-MHz Bruker Avance DPX spectrometer. FT-IR spectra were recorded on a Nicolet Impact 400D infrared spectrometer. Elemental analyses were done using a Perkin Elmer Series II 2400 CHN analyzer. The electronic absorption spectra were recorded on a Shimadzu 3101PC UV-vis-NIR scanning spectrophotometer. Steady-state fluorescence measurements were performed with a SPEX Fluorolog F112X spectrofluorometer. All fluorescence spectra were corrected for detector response. The fluorescence quantum yields were determined by the relative method using optically matched solutions. Quinine sulfate in 1 N sulfuric acid ($\Phi_f = 0.546$) was used as the standard. Fluorescence lifetimes were determined using a Edinburgh FL900CD single photon counting system, and the data were analyzed by Edinburgh software. For the fluorescence measurements, concentration of solutions used was in the range of $(3\text{--}5) \times 10^{-6}$ M. The pH measurements were carried out using an ELICO Model L1-120 Digital pH meter, which was calibrated using standard aqueous solutions of pH 4 and 9.2. For every step of the pH titration, small amounts of 11.6 M (37 wt %) HCl were added to solutions of **1** or **2** (50 mL) in a methanol–water (4:1) mixture. All the experiments were carried out at room temperature (298 K).

Materials

The synthesis of **1–5** is reported in the Supporting Information. Spectroscopic and analytical data for **1** and **2** are given here.

Data for 1. Mp 111–112 °C. ^1H NMR (CDCl_3 , 300 MHz): δ 1.46 (t, 3H, CH_3), 2.86–2.87 (m, 8H, benzylic), 2.99 (s, 6H, $\text{N}(\text{CH}_3)_2$), 4.36 (q, 2H, CH_2), 6.45 (s, 2H, ArH), 7.71 (s, 2H, ArH). ^{13}C NMR (CDCl_3): δ 14.42, 28.35, 28.9, 40.46, 60.56, 109.7, 118.12, 126.58, 126.99, 133.5, 135.82, 137.48, 150.58, 167.08. IR (KBr): 2927, 2888, 2831, 1713, 1596, 1483, 1438, 1365, 1292, 1197 cm^{-1} . Anal. Calcd. for $\text{C}_{21}\text{H}_{23}\text{NO}_2$: C, 78.47; H, 7.21; N, 4.36. Found: C, 78.62; H, 7.13; N, 4.65.

Data for 2. Mp 144–145 °C. ^1H NMR (CDCl_3 , 300 MHz): δ 2.8 (s, 8H, benzylic), 3.0 (s, 6H, $\text{N}(\text{CH}_3)_2$), 6.45 (s, 2H, ArH), 7.28 (s, 2H, ArH). ^{13}C NMR (CDCl_3): δ 28.04, 28.45, 40.27, 107.18, 109.57, 118.0, 120.0, 129.20, 134.14, 135.89, 137.38, 150.78. IR (KBr): 2949, 2893, 2831, 2208, 1584, 1433, 1376, 1365 cm^{-1} . Anal. Calcd. for $\text{C}_{19}\text{H}_{18}\text{N}_2$: C, 83.17; H, 6.61; N, 10.21. Found: C, 83.55; H, 6.59; N, 10.05.

Results and Discussion

Absorption Spectra. The absorption spectra of **1** and **2** in cyclohexane and acetonitrile in the 230–500-nm region are

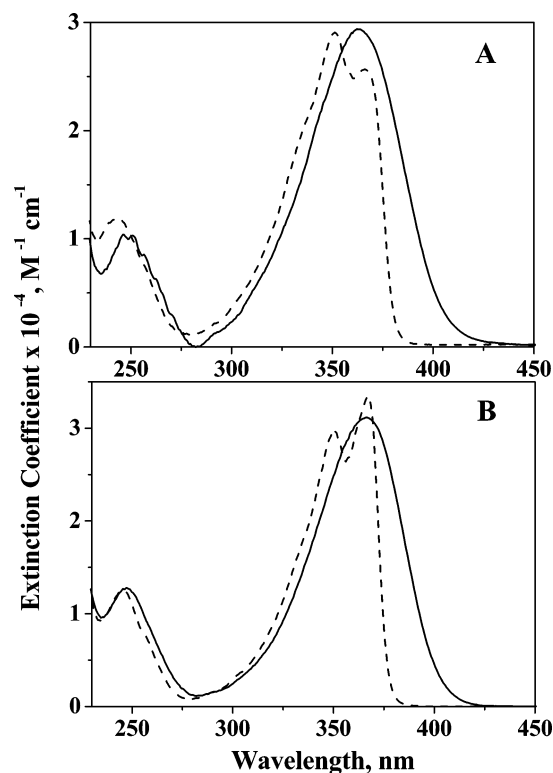
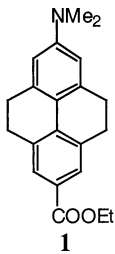
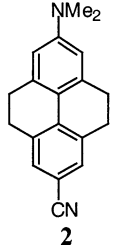


Figure 1. Absorption spectra of (A) **1** and (B) **2** in cyclohexane (dashed line) and acetonitrile (solid line) at 298 K.

given in Figure 1. The spectra in cyclohexane exhibit fine structure, which for biphenyl derivatives suggests absence of free rotation about the $\text{C}_1 - \text{C}_1'$ bond.⁴⁶ The absorption spectra of **1** and **2** in cyclohexane also provide useful information regarding the electronic nature (^1A or ^1B symmetry) of the Franck–Condon (FC) states. Coggeshall and Pozefsky⁴⁷ have pointed out that absorption spectra involving transitions to 1L_a states in biphenyls generally have vibrational spacing of 1300 cm^{-1} and spectra involving transitions to 1L_b states have vibrational spacing of 1000 cm^{-1} . The vibrational spacings for the absorption of **1** and **2** in cyclohexane were 1242 and 1323 cm^{-1} , respectively. On the basis of the observed vibrational spacing, the lowest-energy transitions in **1** and **2** can be assigned to the $^1\text{A} \rightarrow ^1L_a$ transition. In polar solvents, the absorption bands of **1** and **2** are slightly broadened relative to that in cyclohexane, and the fine structure is lost, but the absorption maxima varied only slightly (Table 1). The integrated absorption intensity $\int \epsilon \, d\nu_a$, which is proportional to the oscillator strength f , changes only slightly with solvent polarity (Table 1). This suggests that the electronic and structural nature of the ground and FC excited states responsible for these absorptions do not vary much with solvent polarity.

Tetrahydropyrenes **1** and **2** are analogous to D–A biphenyls, where the excitation leads to CT from the dimethylaminophenyl moiety to the carbomethoxyphenyl or cyanophenyl unit. To look into this process in detail, we have studied the model compounds **3–5** where such CT processes cannot occur. The absorption spectra of model compounds **3–5** in cyclohexane are shown in Figure 2A. A comparison of the absorption spectra of **1** and **2** with the model compounds showed that the maximum of the first absorption band of **1** (or **2**) is located at ~ 3300 and 4200 cm^{-1} to the red of the corresponding bands in the model compounds **3** and **4** (or **5**). Absorption spectra of **1** and **2** exhibited significant changes in the presence of trifluoroacetic acid (TFA). The effect of addition of TFA on the absorption spectrum of **2** in cyclohexane is shown in Figure 2B. The

TABLE 1: Spectroscopic Data for **1** and **2** in Various Solvents

compound	solvent	$\lambda_{a, \max}$, nm	$f \epsilon d\nu_a$, $10^8 \text{ M}^{-1} \text{ cm}^{-2}$	$\lambda_{f, \max}$, nm	ν_{st} , 10^3 cm^{-1}
 1	cyclohexane	351, 366	1.01	375, 396	2.37
	benzene	359	1.19	421	4.14
	toluene	359	1.16	418	3.92
	diisopropyl ether	355	1.25	423	4.53
	tetrahydrofuran	363	1.30	440	4.87
	dichloromethane	365	1.12	444	4.91
	ethyl acetate	359	1.31	432	4.71
	acetonitrile	362	1.18	472	6.43
	methanol	359	1.36	503	7.70
 2	cyclohexane	350, 367	1.12	377, 392	1.73
	benzene	369	1.12	417	3.12
	toluene	370	1.10	418	3.14
	diisopropyl ether	365	1.09	417	3.45
	tetrahydrofuran	369	1.19	430	3.88
	dichloromethane	369	1.11	430	3.90
	ethyl acetate	365	1.25	424	3.85
	acetonitrile	367	1.18	442	4.67
	methanol	367	1.25	453	5.21

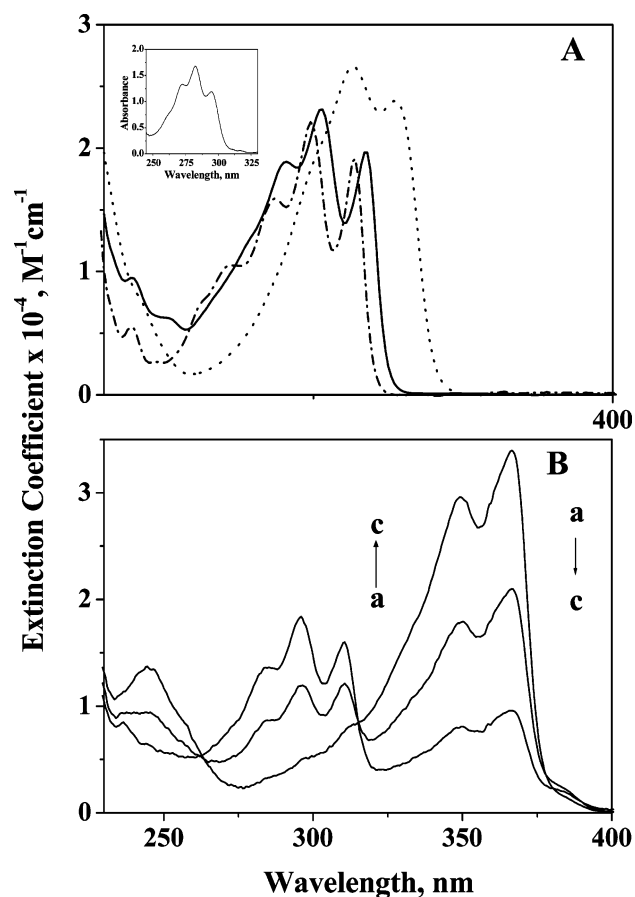


Figure 2. (A) Absorption spectra at 298 K of model compounds **3** (dotted line), **4** (solid line) and **5** (dot-dashed line) in cyclohexane and (B) change in the absorption spectrum of **2** in cyclohexane with varying concentrations of TFA. [TFA]: (a) = 0.0 mM; (b) = 0.5 mM; and (c) = 2.2 mM. The insert in 2A is the absorption spectrum of unsubstituted tetrahydropyrene at 298 K.

intensity of the 360-nm band decreases with simultaneous formation of a new band around 300 nm. This new band is identical to the absorption spectrum of model compound **5**. TFA protonates the dimethylamino group in **2**. The longest conjugated chromophore in protonated **2** is the same as that in **5**. Figure 2 shows that addition of a dimethylamino group to **5** results in a

redshift of 53 nm. Whether this redshift is due to extended conjugation alone or if a CT process is also involved is to be examined. This is done by comparing the 0–0 band positions in **2** (367 nm), **3** (327 nm), and **5** (314 nm) with the 0–0 band position in unsubstituted tetrahydropyrene (294 nm, inset of Figure 2A). It can be seen that substitutions of cyano and dimethylamino groups lead to redshifts of 20 and 33 nm, respectively. On this basis, one would expect a redshift of 53 nm for the 0–0 band of **2** (compared to unsubstituted tetrahydropyrene). The actual redshift observed was 73 nm, which suggests that, in addition to extended conjugation, a CT process also contributes to the red shift. The same arguments hold true for **1** also. We thus conclude that the lowest energy transition in **1** and **2** have strong CT character.

Fluorescence Spectra. Fluorescence spectra of **1** and **2** in various solvents are shown in Figure 3. In cyclohexane, fluorescence spectra of both compounds exhibit vibrational structure, which indicate that emission is taking place from a planar state.⁴⁶ Since the ground states are twisted by 14°, this suggests a structural relaxation to planarity in the excited states of **1** and **2**. Structural relaxation is further confirmed from the intensity ratios of the first and second vibronic bands in the fluorescence spectra in cyclohexane. The ratio is nearly 1:1 in both cases, which suggests that the minima of the ground and excited states are somewhat displaced.³³ The vibrational spacings in the fluorescence spectra of **1** and **2** in cyclohexane are $\sim 1270 \text{ cm}^{-1}$. This value is close to the value of $\sim 1300 \text{ cm}^{-1}$ observed for biphenyl derivatives such as 4-vinylbiphenyl, 4-cyanobiphenyl, and *p*-terphenyl.²⁶ For all these compounds, the emitting state is a long axis-polarized 1L_a state, and on the basis of this analogy, we conclude that the fluorescence in **1** and **2** arise due to $^1L_a \rightarrow ^1A$ transitions.³³ The ICT nature of the emitting states is further confirmed from the $>4000 \text{ cm}^{-1}$ redshift of the fluorescence spectra of **1** and **2** compared to those of the model compounds **3–5**.

The fluorescence spectra of **1** and **2** in dipolar solvents are structureless and exhibit solvatochromic redshifts with increasing solvent polarity. The absorption and fluorescence maxima of **1** and **2** in various solvents along with the observed Stokes shift values are presented in Table 1. (Wherever the absorption/fluorescence spectra exhibited structure, the 0–0 band maxima were used for calculating Stokes shift. In other cases, the band

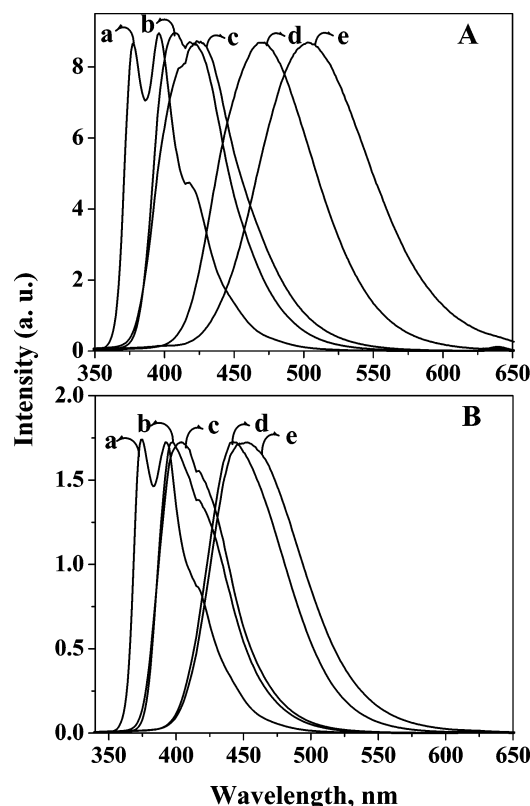


Figure 3. Normalized fluorescence spectra of (A) **1** and (B) **2** at 298 K in various solvents: (a) cyclohexane, (b) toluene, (c) diisopropyl ether, (d) acetonitrile, and (e) methanol.

maxima were used for this calculation.) The Stokes shifts observed for **1** and **2** are larger than those observed for 2-(dimethylamino)-7-cyanofluorene ($\varphi = 0^\circ$) and smaller than those observed for 4-(dimethylamino)-4'-cyanobiphenyl ($\varphi = 39^\circ$).³³ This also supports the small geometric relaxation to planarity taking place in the excited states of **1** and **2**.

Solvent-dependent shifts in the fluorescence spectra can be attributed to factors such as (1) dipole–dipole interactions between solvent and solute, (2) changes in the nature of emitting state induced by the solvent, and (3) specific solvent–solute interactions such as hydrogen bonding. To have a better understanding of the excited states of **1** and **2**, we have tried to correlate the observed Stokes shifts to the Dimroth $E_T(30)$ parameter⁴⁸ and the fluorescence maxima to the Kamlet–Taft π^* scale.⁴⁹ The results are plotted in Figure 4. In both cases, the plots were linear with correlation coefficients $r = 0.92$ and 0.90 , respectively. Linearity of these plots suggest that dipole–dipole interactions between the solute and solvent are responsible for the large solvent-dependent shifts observed for the fluorescence spectra of **1** and **2**.^{48,49}

The solvatochromic Stokes shifts were further analyzed to obtain quantitative information about the dipole moments of the fluorophores. The Lippert–Mataga equation^{50,51} was used for this purpose

$$\nu_{st} = 2(\mu_e - \mu_g)^2 \Delta f / hca^3 + C \quad (1)$$

where

$$\Delta f = [(\epsilon - 1)/(2\epsilon + 1)] - [(n^2 - 1)/(2n^2 + 1)] \quad (2)$$

In the equations, μ_e and μ_g are the excited- and ground-state dipole moments respectively, h is the Planck's constant, c is the velocity of light, a is the radius of the cavity in which the

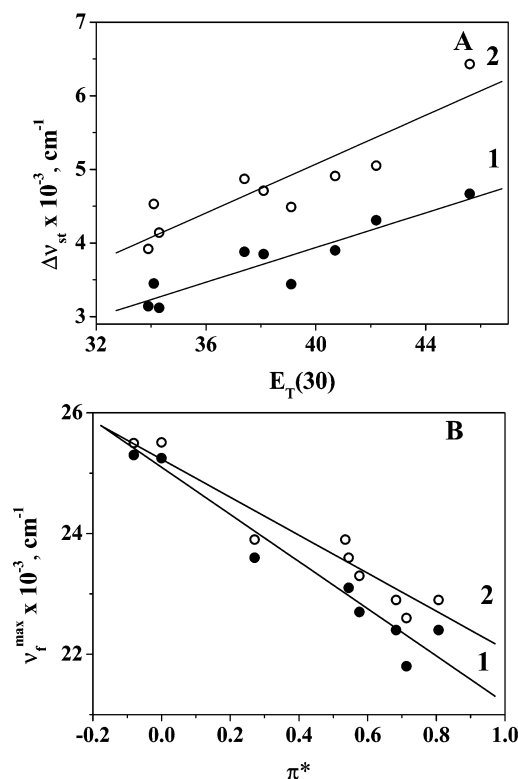


Figure 4. Plots of (A) Stokes shift values vs $E_T(30)$ and (B) ν_{\max} vs π^* for **1** and **2**.

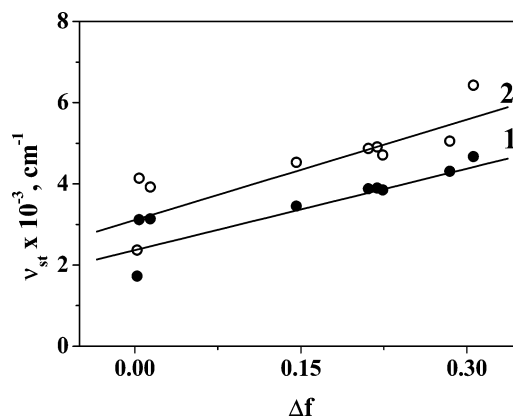
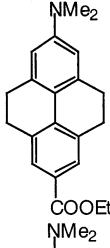
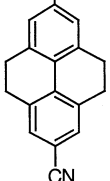


Figure 5. Lippert–Mataga plots for **1** and **2**.

fluorophore resides (Onsager radius), Δf is known as the solvent polarity parameter, and ϵ and n are the dielectric constant and refractive index, respectively, of the medium. Δf values for the various solvents were calculated from known values of ϵ and n . The Stokes shift values for **1** and **2** were plotted against Δf in Figure 5. From the slopes of these plots, the dipole moments of **1** and **2** in the excited states can be calculated if values of a and μ_g are known. The ground-state dipole moments of **1** and **2** were obtained from the AM1 method as 4.02 and 5.81 D, respectively. For both compounds, the Onsager radius was taken as equal to 6.0×10^{-10} m, which is the value reported for several other D–A biphenyls.^{31–33} The excited-state dipole moments thus obtained for **1** and **2** were 20.4 and 20.1 D, respectively. These values are similar to those observed for D–A biphenyls and D–A fluorenes.³³ The high values of μ_e show that significant CT occurs for **1** and **2** in the excited state.

The Lippert–Mataga treatment as described above assumes that the fluorescence arises from the FC state reached directly after excitation. In the present case, we invoke a planarization

TABLE 2: Photophysical Data for **1** and **2**

compound	solvent	Φ_f	τ_f , ns	k_r , 10^8 s^{-1}	k_{nr} , 10^8 s^{-1}	$k_r^{(SB)}$, 10^8 s^{-1}	$k_r/k_r^{(SB)}$
	cyclohexane	0.54	1.59	3.4	2.8	3.4	1.00
	dichloromethane	0.62	2.26	2.8	1.6	2.5	1.08
	ethyl acetate	0.68	1.97	3.4	1.6	3.3	1.04
	acetonitrile	0.61	2.41	2.5	1.6	2.2	1.13
	methanol	0.80	2.78	2.9	0.6	2.1	1.25
	cyclohexane	0.60	1.77	3.4	2.2	3.1	1.09
	dichloromethane	0.54	2.10	2.5	2.2	2.5	1.04
	ethyl acetate	0.64	1.87	3.4	1.9	3.3	1.03
	acetonitrile	0.60	2.20	2.7	1.7	2.6	1.03
	methanol	0.77	2.34	3.3	0.9	3.3	1.00

of the FC state before emission. According to Mataga et al.⁵¹ and Liptay,⁵² the solvatochromic shift of the emission spectra should be used for estimating the excited-state dipole moment μ_e' in such cases. In this modification, the fluorescence maxima are correlated to the solvent polarity parameter $\Delta f'$ according to eqs 3 and 4

$$\nu_f = -2\mu_e'(\mu_e' - \mu_g)\Delta f'/hca^3 + C \quad (3)$$

where

$$\Delta f' = [(\epsilon - 1)/(2\epsilon + 1)] - 0.5[(n^2 - 1)/(2n^2 + 1)] \quad (4)$$

The excited-state dipole moment μ_e' can be obtained from a plot of ν_f vs $\Delta f'$. This treatment gave values of 20.3 and 19.5 as excited-state dipole moments for **1** and **2**. It is to be noted that values of excited state dipole moments obtained by this treatment are slightly lower.

Fluorescence Quantum Yields and Lifetimes. The fluorescence quantum yields (Φ_f) and lifetimes (τ_f) of **1** and **2** were measured in several solvents. By use of Φ_f and τ_f , the radiative ($k_r = \Phi_f/\tau_f$) and nonradiative ($k_{nr} = (1 - \Phi_f)/\tau_f$) rates were calculated. Values of Φ_f , τ_f , k_r , and k_{nr} for **1** and **2** in several solvents are presented in Table 2. An inspection of Table 2 shows that the fluorescence quantum yields and lifetimes show a relatively wide variation with solvent. For example, the fluorescence quantum yield of **1** changes by nearly 50% upon changing the solvent from cyclohexane to methanol. On this basis, it can be argued that changes in the nature of the excited states or other specific solvent–solute interactions may be taking place in these systems. The issue can be resolved qualitatively in the following manner.

The radiative rate constant k_r is given by eq 5^{33,56,57}

$$k_r = \frac{64\pi^4}{3h} n^3 \nu_f^3 M_f^2 \quad (5)$$

where M_f is the fluorescence transition moment. A change of the electronic or molecular structure between the absorption and fluorescence process can be evaluated by a comparison of the radiative rate constant k_r with the natural fluorescence lifetime (Strickler–Berg rate constant, $k_r^{(SB)}$). $k_r^{(SB)}$ can be calculated from the absorption spectrum using eq 6

$$k_r^{(SB)} = \frac{8\pi c}{N_L} \frac{10^3 \ln 10}{n^2 \nu_f^3} \int \epsilon(\nu_a) d \ln \nu_a \quad (6)$$

where N_L is the Loschmidt's constant (Avogadro's number). The value of the integrated absorption is given by^{33,56–58}

$$\int \epsilon(\nu_a) d \ln \nu_a = \frac{8\pi^3 N_L n}{3hc \cdot 10^3 \ln 10} M_a^2 \quad (7)$$

where M_a is the absorption transition moment. By substitution of eq 7 in to eq 6, we get

$$k_r^{(SB)} = \frac{64\pi^4}{3h} n^3 \nu_f^3 M_a^2 \quad (8)$$

Dividing eq 5 by eq 8

$$\frac{k_r}{k_r^{(SB)}} = \frac{M_f^2}{M_a^2} \quad (9)$$

If no change of electronic or molecular structure takes place in S_1 , $M_a = M_f$, and hence, $k_r/k_r^{(SB)} = 1$.

To see if there is any change in the nature of the excited states upon changing the solvent, we have calculated $k_r^{(SB)}$ for **1** and **2** in several solvents and the results are given in Table 2. For this calculation, the absorption spectrum $\epsilon(\nu_a)$ was fitted to a Gaussian function. Values of $k_r/k_r^{(SB)}$ were then calculated, and these are also given in Table 2. In all solvents, values of $k_r/k_r^{(SB)}$ for **1** and **2** were very close to unity, suggesting that the geometric relaxation taking place in the excited state is very small. Also, $k_r/k_r^{(SB)}$ values are similar in all solvents, which indicates that the emitting state is the same in all solvents studied.

It is to be mentioned that calculation of $k_r^{(SB)}$ by eq 6 assumed that the absorption band over which the integration is performed consisted only of the transition leading to fluorescence and that the nuclear configuration of the chromophore did not change appreciably on excitation. Although we have not detected contributions due to any other transitions in the low-energy absorption bands of **1** and **2**, planarization occurs in the excited state, leading to a difference in the nuclear configurations of the two states. This conclusion derived from eq 9 is only qualitative in the present case.

The photophysical properties of tetrahydropyrene derivatives **1** and **2** are in good agreement with those of 4-*N*,*N*-dimethylamino-4'-cyanobiphenyl and 4-*N*,*N*-dimethylamino-4'-cyano-fluorene, studied in detail by Rettig, Maus, and co-workers.^{33–37} These compounds exhibited high fluorescence quantum yields

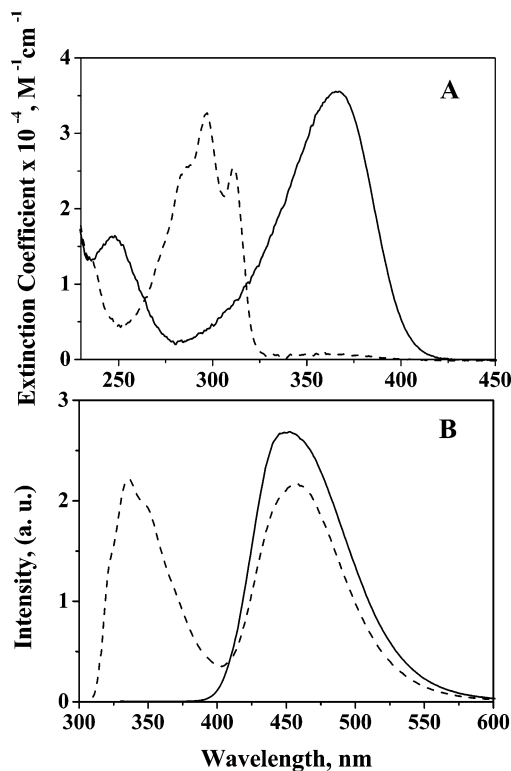


Figure 6. Effect of protons on (A) the absorption and (B) emission spectra of **2** in methanol at 298 K. The solid line denotes the spectrum in methanol, and the dotted line denotes the spectrum after the addition of acid.

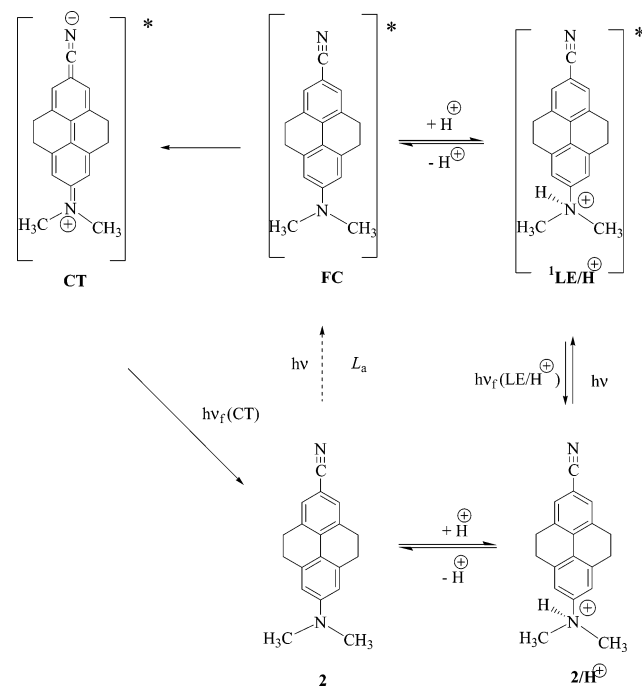
(0.57–0.81) and short fluorescence lifetimes (1.4–2.1 ns), and these properties were relatively insensitive to changes in solvent polarity. The authors suggested that, independent of the ground-state twist angle (φ) and solvent polarity, the first excited singlet state in all these D–A systems is a planar, emissive intramolecular ^1CT of the 1L_a type, transferring charge from the dimethylaminobenzene donor moiety to the cyanobenzene acceptor moiety. This is in contrast to the behavior of 4-*N,N*-(dimethylamino)-2,6-dimethyl-4'-cyanobiphenyl ($\varphi = 78^\circ$) for which fluorescence quantum yields and lifetimes depended on solvent polarity. A fast equilibrium between a more planar and more twisted rotamer distribution in the ^1CT state is invoked to explain the photophysics in this case. Twisting of the dimethylamino moiety with respect to the phenyl group with which it is attached is not active in promoting nonradiative transition in any of these cases.

Effect of Added Protons. The absorption and fluorescence spectra of **1** and **2** undergo drastic changes in the presence of added protons. Figure 6A shows the absorption spectra of **2** in MeOH and MeOH/ H^+ ($[\mathbf{2}] = 4 \times 10^{-5} \text{ M}$, $[\text{HCl}] = 0.1 \text{ M}$). Addition of H^+ leads to disappearance of the absorption band at 366 nm and formation of a new band at 297 nm. Figure 6B shows the fluorescence spectra of **2** in MeOH and MeOH/ H^+ . The absorption and emission in the absence of H^+ can be assigned to the ^1CT state described earlier. In the presence of added acid, a new band is formed at 297 nm and this can be attributed to the protonated form. The emission spectrum in the presence of H^+ exhibited bands at 336 and 457 nm. The 457-nm band is identical to the band observed in the absence of H^+ and is attributed to the ^1CT band, and hence, the band at 336 nm was attributed to the protonated form. The assignment of the new absorption and emission bands to the protonated state is confirmed by comparing these to the corresponding spectra of the model compound **5**. This also confirmed that protonation

TABLE 3: Absorption and Emission Maxima and $\text{p}K_a^* - \text{p}K_a$ Values for **1 and **2** in Methanol and Methanol/Water Mixture**

compound	solvent	λ_a^{max} , nm		λ_f^{max} , nm		$\text{p}K_a^* - \text{p}K_a$
		LE/ H^+	CT	LE/ H^+	CT	
1	MeOH	299	364	346	504	−15.0
	MeOH/ H_2O	301	358	355	528	−15.3
2	MeOH	297	366	336	457	−15.0
	MeOH/ H_2O	298	361	339	477	−15.5

SCHEME 1



occurs at the dimethylamino group leading to elimination of the CT process. In the remaining section of this manuscript, this state is referred to as $^1\text{LE}/\text{H}^+$ state.

Figure 6 shows that in the presence of excess acid, the ^1CT absorption band disappears. This means that only the protonated forms exist in S_0 , and hence, the CT band seen in the emission spectrum cannot be arising from direct excitation of the CT band. Therefore, the CT fluorescence band should be arising due to excited-state deprotonation, as is reported for a few other D–A biphenyl derivatives.⁵³ Facile deprotonation can occur in the excited state if the excited state is more acidic than the ground state. The difference in the $\text{p}K_a$ values of the excited and ground states can be calculated using eq 10^{53–55}

$$\text{p}K_a^* - \text{p}K_a = \frac{hc}{kT \ln 10} \left(\frac{\nu_a(\text{CT}) + \nu_f(\text{CT})}{2} - \frac{\nu_a(\text{LE}/\text{H}^+) + \nu_f(\text{LE}/\text{H}^+)}{2} \right) \quad (10)$$

Values of $\text{p}K_a^* - \text{p}K_a$ thus calculated for **1** and **2** in MeOH and 4:1 MeOH/ H_2O are given in Table 3. These values are highly negative. Taking into account the small ground-state $\text{p}K_a$ values (vide infra), we can conclude that protonated **1** and **2** exhibit highly negative $\text{p}K_a^*$ values, which point to a strong driving force for deprotonation in the excited state for these compounds.

On the basis of the studies presented so far, the photoinduced processes in **2** in methanol in the presence of H^+ can be described as shown in Scheme 1. In the ground state, the

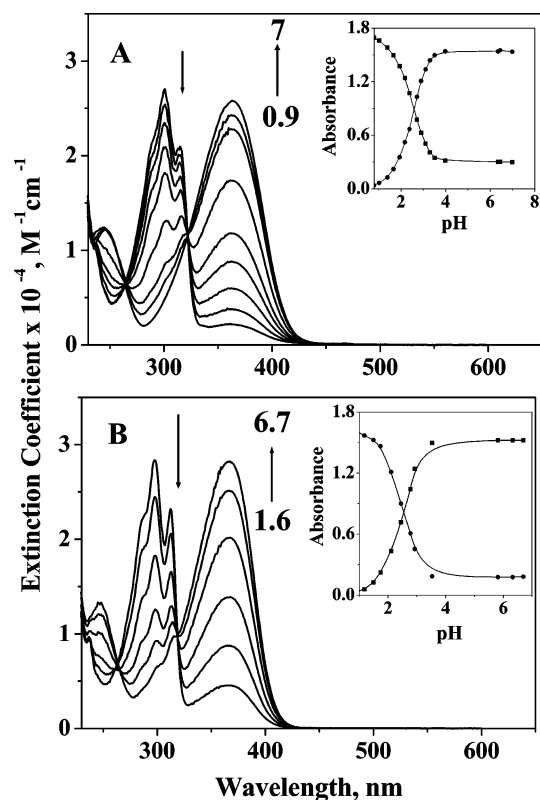


Figure 7. pH-dependent absorption spectra of (A) **1** and (B) **2** in 4:1 MeOH/H₂O at 298 K. Insets show the titration curves.

equilibrium is in favor of the protonated state. Excitation leads to formation of the LE/H⁺ excited state. This state can undergo emission, leading to the formation of the LE/H⁺ band, or undergo excited-state deprotonation. The deprotonated state immediately rearranges to the planar, delocalized CT state, which can undergo emission to the ground state, thereby giving rise to the CT band in the emission spectrum. In the absence of protons, excitation leads to the FC state (dotted arrow), which undergoes planarization and delocalization to the CT state, from which emission takes place. A similar mechanism is occurring in the case of **1**.

In Scheme 1, direct excitation of **2** leads to the formation of the FC species. This state is also populated by the deprotonation of the ¹LE/H⁺ state. Only indirect evidence can be presented at this time for the existence of the FC state. Steady-state fluorescence spectra or nanosecond-lifetime data did not give direct evidence for the FC state. Investigations by Rettig and co-workers³⁵ on differently twisted biphenyl derivatives using picosecond-absorption technique revealed the presence of a very short-lived FC state ($\tau = 2.5$ ps) in these systems. Thus, in all probability, the FC state, which acts as a precursor to the CT state, has a sub-nanosecond lifetime and could not be detected in the nanosecond time window.

The basic emission features of **1** and **2** in acidic methanol indicate the possibility of using these systems as dual-emissive, ratio-able fluorescent probes.⁵³ To test the potential of these compounds in pH sensing applications, pH-dependent absorption and emission studies were carried out in 4:1 methanol/water system. The changes observed in the absorption spectra of **1** and **2** as a function of pH are shown in Figure 7. As the pH is changed from 6.7 to 1.5, the absorption in the 360-nm region decreases with simultaneous increase in the new absorption around 297 nm. The isosbestic points in the absorption spectra reflect the ground-state acid–base equilibrium involving the protonated and nonprotonated species. The spectrophotometric

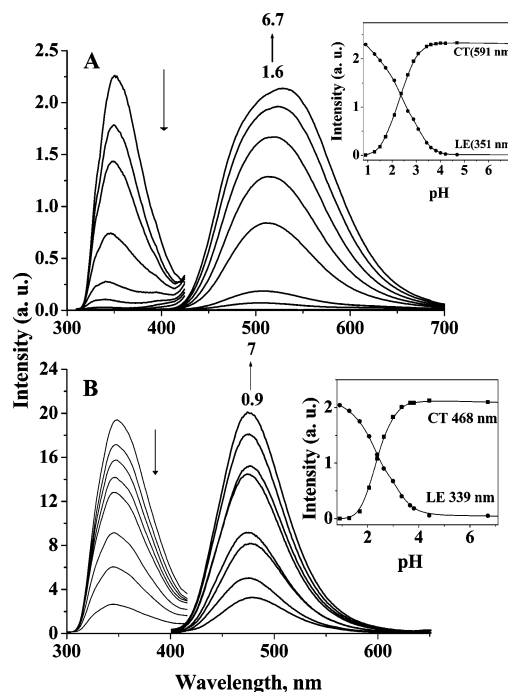


Figure 8. pH-dependent fluorescence spectra for (A) **1** and (B) **2** in 4:1 MeOH/H₂O at 298 K. Insets show the titration curves.

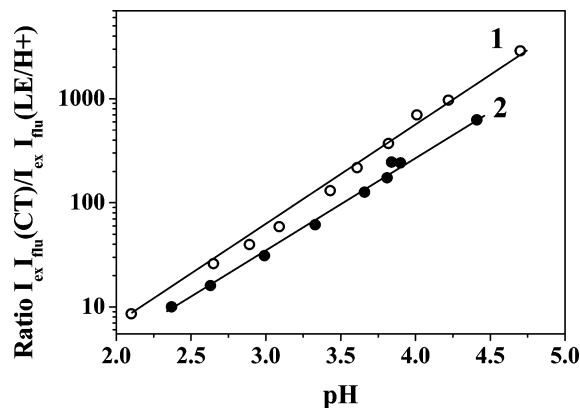


Figure 9. pH calibration curves for **1** and **2**.

titration curves are shown in the inset. From the inflection points in the titration curves, pK_a values of 2.6 and 2.55 were determined for **1** and **2**, respectively.

Changes observed in the emission spectra of **1** and **2** as a function of pH are shown in Figure 8. The titration curves are given as inset in the figure. From the inflection points in the fluorescence titration curves, the pK_a values obtained were 2.4 and 2.5, respectively, for **1** and **2**. pK_a values obtained by this method are very close to the values obtained from the spectrophotometric titration curves.

The above studies show that, in the pH range of 1–4, tetrahydropyrenes **1** and **2** exhibit two well-separated strong absorption bands and two well-separated emission bands. This property makes them ideally suited for pH-sensing applications, in this pH range. For **1** and **2**, the ratio of the emission intensities $I_{\text{ex}} I_{\text{em}}(\text{CT})/I_{\text{ex}} I_{\text{em}}(\text{LE/H}^+)$, where $I_{\text{ex}} I_{\text{em}}(\text{CT})$ represents the maximum intensity of the CT emission obtained by excitation at the CT absorption maxima and $I_{\text{ex}} I_{\text{em}}(\text{LE/H}^+)$ represents the maximum intensity of the emission obtained by excitation at the LE/H⁺ absorption maxima, spans a range of 3 orders of magnitude. In Figure 9, this ratio is plotted against pH. It can be seen from the figure that plots of $I_{\text{ex}} I_{\text{em}}(\text{CT})/I_{\text{ex}} I_{\text{em}}(\text{LE/H}^+)$ vs pH are linear

with correlation > 0.99 . Since the ratio spans a range of 3 orders of magnitude, the plot can serve as a highly sensitive calibration curve for pH determinations in the range of pH 1–4.

Conclusions

Photoinduced intramolecular CT processes in the tetrahydro-pyrene derivatives **1** and **2** were probed by absorption and emission techniques. These molecules are slightly twisted at the central C₁–C₁' bond in the ground state. The absorption maxima did not exhibit any solvent dependence, indicating that the electronic structure of the ground state is similar in all solvents and that the excitation is a $^1A \rightarrow ^1L_a(CT)$ transition. The FC ICT states undergo relaxation to a planar state, which facilitate extended conjugation and CT from the donor dimethylaminophenyl to the acceptor cyanophenyl or carbomethoxyphenyl groups. The emission in **1** and **2** arises as a result of $^1L_a(CT) \rightarrow ^1A$ transition. The CT states are stabilized in polar solvents, leading to redshifts in the fluorescence spectra. Changes in the fluorescence maxima of **1** and **2** were correlated to the Kamlet–Taft π^* scale, and the solvent-dependent Stokes shifts were correlated to the Dimroth $E_T(30)$ parameter. These were further quantitatively analyzed using the Lippert–Mataga equation and Liptay's modified equation. In the presence of proton acids, **1** and **2** exhibit pH-dependent dual absorption and dual emission, and this property can be exploited to design highly sensitive, ratiometric fluorescent pH probes.

Acknowledgment. The authors wish to thank the Council of Scientific and Industrial Research (CSIR), Government of India and the Department of Science and Technology (DST), Government of India, for financial support.

Supporting Information Available: A detailed synthetic scheme (Scheme 1S) and experimental procedures are given in the Supporting Information. This material is available via the Internet at <http://pubs.acs.org>.

References and Notes

- (1) Zhang, X.; Wang, C.-J.; Liu, L.-H.; Jiang, Y.-B. *J. Phys. Chem. B* **2002**, *106*, 12432.
- (2) Fayed, T. A.; Organero, J. A.; Garcia-Ochoa, I.; Tormo, L.; Douhal, A. *Chem. Phys. Lett.* **2002**, *364*, 108.
- (3) Hazra, P.; Chakrabarthy, D.; Sarkar, N. *Langmuir* **2002**, *18*, 7872.
- (4) Maliakal, A.; Lem, G.; Turro, N. J.; Ravichandran, R.; Suhadolnik, J. C.; DeBellis, A. D.; Wood, M. G.; Lau, J. *J. Phys. Chem. A* **2002**, *106*, 7680.
- (5) Das, S. K. *Chem. Phys. Lett.* **2002**, *361*, 21.
- (6) Zachariasse, K. A.; Yoshihara, T.; Druzhinin, S. I. *J. Phys. Chem. A* **2002**, *106*, 6325.
- (7) Chattopadhyay, N.; Serpa, C.; Arnaut, L. G.; Formosinho, S. J. *Helv. Chim. Acta* **2002**, *85*, 19.
- (8) Huang, W.; Zhang, X.; Ma, L.-H.; Wang, C.-J.; Jiang, Y.-B. *Chem. Phys. Lett.* **2002**, *352*, 401.
- (9) Zilberg, S.; Haas, Y. *J. Phys. Chem. A* **2002**, *106*, 1.
- (10) Lee, J. Y.; Kim, K. S.; Mhin, B. J. *J. Chem. Phys.* **2001**, *115*, 9484.
- (11) Druzhinin, S. I.; Demeter, A.; Zachariasse, K. A. *Chem. Phys. Lett.* **2001**, *347*, 421.
- (12) Chattopadhyay, N.; Serpa, C.; Pereira, M. M.; Seixas de Melo, J.; Arnaut, L. G.; Formosinho, S. J. *J. Phys. Chem. A* **2001**, *105*, 10025.
- (13) Parusel, A. B. *J. Chem. Phys. Lett.* **2001**, *340*, 531.
- (14) Demeter, A.; Berces, T.; Zachariasse, K. A. *J. Phys. Chem. A* **2001**, *105*, 4611.
- (15) Singh, A. K.; Kanvah, S. *J. Chem. Soc., Perkin Trans. 2* **2001**, 395.
- (16) Herbich, J.; Brutschy, B. In *Electron-Transfer Chemistry*; Balzani, V., Ed.; Wiley-VCH: Weinheim, 2001; Vol. 4, pp 697–741.
- (17) Dobkowski, J.; Wojcik, J.; Kozminski, W.; Kolos, R.; Waluk, J.; Michl, J. *J. Am. Chem. Soc.* **2002**, *124*, 2406.
- (18) Parusel, A. B. J.; Rettig, W.; Sudholt, W. *J. Phys. Chem. A* **2002**, *106*, 804.
- (19) Rettig, W.; Lutze, S. *Chem. Phys. Lett.* **2001**, *341*, 263.
- (20) Mennucci, B.; Toniolo, A.; Tomasi, J. *J. Am. Chem. Soc.* **2000**, *122*, 10621.
- (21) von der Haar, T.; Hebecker, A.; Il'ichev, Y.; Jiang, Y. B.; Kühnle, W.; Zachariasse, K. A. *Recl. Trav. Chim. Pays-Bas* **1995**, *114*, 430.
- (22) Zachariasse, K. A.; von der Haar, T.; Hebecker, A.; Leinhos, U.; Kühnle, W. *Pure Appl. Chem.* **1993**, *65*, 1745.
- (23) Sobolewski, A. L.; Domcke, W. *Chem. Phys. Lett.* **1996**, *259*, 119.
- (24) Rettig, W. *Angew. Chem., Int. Ed. Engl.* **1986**, *25*, 971.
- (25) Grabowski, Z. R.; Rotkiewicz, K.; Siemiarczuk, A.; Cowley, D. J.; Baumann, W. *Nouv. J. Chim.* **1979**, *3*, 443.
- (26) Momicchioli, F.; Bruni, M. C.; Baraldi, I. *J. Phys. Chem.* **1972**, *76*, 3983.
- (27) Kurland, R.; Wise, W. B. *J. Am. Chem. Soc.* **1964**, *86*, 1877.
- (28) Eaton, V. J.; Steele, D. *J. Chem. Soc., Faraday Trans. 2* **1973**, *69*, 1601.
- (29) Takei, Y.; Yamaguchi, T.; Osamura, Y.; Fuke, K.; Kaya, K. *J. Phys. Chem.* **1988**, *92*, 577.
- (30) Butler, R. M.; Lynn, M. A.; Gustafson, T. L. *J. Phys. Chem.* **1993**, *97*, 2609.
- (31) Lahmani, F.; Breheret, E.; Zehnacker-Rentien, A.; Amatore, C.; Jutand, A. *J. Photochem. Photobiol., A* **1993**, *70*, 39.
- (32) Lahmani, F.; Breheret, E.; Benoist d'Azy, O.; Zehnacker-Rentien, A.; Delouis, J. F. *J. Photochem. Photobiol., A* **1995**, *89*, 191.
- (33) Maus, M.; Rettig, W.; Bonafoux, D.; Lapouyade, R. *J. Phys. Chem. A* **1999**, *103*, 3388.
- (34) Maus, M.; Rettig, W. *Chem. Phys.* **1997**, *218*, 151.
- (35) Maus, M.; Rettig, W.; Jonusauskas, G.; Lapouyade, R.; Rullière, C. *J. Phys. Chem. A* **1998**, *102*, 7393.
- (36) Maus, M.; Rettig, W. *Chem. Phys. Lett.* **2000**, *324*, 57.
- (37) Rettig, W.; Kharlanov, V.; Maus, M. *Chem. Phys. Lett.* **2000**, *318*, 173.
- (38) Herbich, J.; Waluk, J. *Chem. Phys.* **1994**, *188*, 247.
- (39) Klock, A. M.; Rettig, W. *Pol. J. Chem.* **1993**, *67*, 1375.
- (40) Maus, M.; Rettig, W.; Lapouyade, R. *J. Inf. Rec. Mater.* **1996**, *22*, 451.
- (41) Rettig, W.; Maus, M. *Ber. Bunsen-Ges. Phys. Chem.* **1996**, *100*, 2091.
- (42) Foley, M. J.; Singer, L. A. *J. Phys. Chem.* **1994**, *98*, 6430.
- (43) Lippert, E. *Ber. Bunsen-Ges. Phys. Chem.* **1957**, *61*, 962.
- (44) Chou, P. T.; Chang, C. P.; Clements, J. H.; Meng-Shin, K. *J. Fluoresc.* **1995**, *5*, 369.
- (45) Cowley, D. J.; O'Kane, E.; Todd, R. S. *J. Chem. Soc., Perkin Trans. 2* **1991**, 1495.
- (46) Lakowicz, J. R. *Principles of Fluorescence Spectroscopy*; Plenum Press: New York, 1983; p 8.
- (47) Coggeshall, N. D.; Pozefsky, A. *J. Chem. Phys.* **1951**, *19*, 980.
- (48) Reichardt, C. *Chem. Rev.* **1994**, *94*, 2319.
- (49) Kamlet, M. J.; Abboud, J. L.; Taft, R. W. *J. Am. Chem. Soc.* **1977**, *99*, 6027.
- (50) Lippert, E. *Z. Naturforsch.* **1955**, *10a*, 541.
- (51) Mataga, N.; Kaifu, Y.; Koizumi, M. *Bull. Chem. Soc. Jpn.* **1956**, *29*, 465.
- (52) Liptay, W. *Z. Naturforsch.* **1965**, *20A*, 1441.
- (53) Maus, M.; Rurack, K. *New J. Chem.* **2000**, *24*, 677.
- (54) Förster, Th. *Z. Elektrochem.* **1950**, *54*, 42.
- (55) Lippert, E. In *Organic Molecular Photophysics*; Birks, J. B., Ed.; Wiley and Sons: London, 1975; Vol. 2, pp 1–29.
- (56) (a) Berlman, I. B.; Steingraber, O. *J. J. Chem. Phys.* **1965**, *43*, 2140.
- (b) Berlman, I. B. *J. Chem. Phys.* **1970**, *52*, 5616.
- (57) Strickler, S. J.; Berg, R. A. *J. Chem. Phys.* **1962**, *37*, 814.
- (58) Birks, J. B. *Photophysics of Aromatic Molecules*; Wiley-Interscience: New York, 1970.